

# Various scenarios for transition to thorium fuel cycle in the Single-fluid Double-zone Thorium Molten Salt Reactor (SD-TMSR)

O. Ashraf<sup>a,b,\*</sup>, Andrei Rykhlevskii<sup>c</sup>, G. V. Tikhomirov<sup>a</sup>, Kathryn D. Huff<sup>c</sup>

<sup>a</sup>*Laboratory of Engineering Computer Modeling in Nuclear Technologies, Institute of Nuclear Physics and Engineering, National Research Nuclear University MEPhI, Moscow, Russia, 115409*

<sup>b</sup>*Physics Department, Faculty of Education, Ain Shams University, Cairo, Egypt, 11341*

<sup>c</sup>*Dept. of Nuclear, Plasma, and Radiological Engineering, University of Illinois at Urbana-Champaign, Urbana, IL 61801, United States*

---

## Abstract

Liquid-fueled Molten Salt Reactor (MSR) systems represent advances in safety, economics, sustainability, and proliferation-resistance. Therefore, Molten Salt Reactor (MSR) has been selected as one of the promising reactors by the Generation IV International Forum (GIF). Basically, the MSR has been designed to operate based on Th/<sup>233</sup>U fuel cycle. Since <sup>233</sup>U does not exist in nature, it is required to examine available fissile materials to replace the <sup>233</sup>U in the startup fuel. Here, five different types of initial fissile materials are proposed for transitioning to thorium fuel cycle in the Single-fluid Double-zone Thorium-based Molten Salt Reactor (SD-TMSR). Plutonium mixed with Low-enriched uranium (LEU) (19.79%), LEU (19.79%), Plutonium reactor-grade, Transuranic elements (TRU) from LWR spent fuel (SF) and finally <sup>233</sup>U for comparison purpose are investigated. In the present paper, two different feed mechanisms are applied. Consequently, the multiplication factor, inventories of important nuclides and net production of <sup>233</sup>U are studied. Moreover, the molten salt Temperature Coefficient of Reactivity ( $\alpha_T$ ) is negative for startup and equilibrium states. The results show that the continuous flow of Pu reactor-grade helps in transition to

---

\*Corresponding Author

Email address: osama.ashraf@edu.asu.edu.eg oabdelaziz@mephi.ru (O. Ashraf)

thorium fuel cycle within a relatively short time ( $\approx 4.5$  years) compared to 26 years for Th/ $^{233}\text{U}$  startup fuel. Meanwhile, using TRU as initial fissile materials shows the possibility of operating the SD-TMSR for a long period of time ( $\approx 40$  years) without any external feed of  $^{233}\text{U}$ .

*Keywords:* MSR, thorium fuel cycle, transmuter, burner, online reprocessing, Monte carlo code

---

## 1. Introduction

The Generation IV International Forum (GIF) has defined eight technology goals for the next generation nuclear systems. These goals are; safety and reliability, economics, sustainability, non-proliferation and physical protection  
5 [1]. Molten Salt Reactors (MSRs) have many advantages that consistent with GIF's goals, for example, liquid fuel, inherent safety, online reprocessing and refueling, excellent neutron economy and operation under ambient pressure [2, 3]. Therefore, in 2002 the MSR has been chosen as one of the promising reactors by this forum [1, 4]. In the MSR, the fuel supposed to be in the form of liquid  
10 dissolved in molten salt (e.g., LiF or NaCl). This liquid fuel salt (e.g., LiF-BeF<sub>2</sub>-ThF<sub>4</sub>- $^{233}\text{U}$ F<sub>4</sub>) constantly circulates through the core and allows transferring fission heat.

The Single-fluid Double-zone Thorium-based Molten Salt Reactor (SD-TMSR-2,250 MWth) was introduced by the Chinese Academy of Sciences (CAS) [5]. The  
15 SD-TMSR is a graphite-moderated thermal-spectrum MSR. In the SD-TMSR the fissile and fertile elements are integrated into the same salt. In addition, the active core is divided into two zones, the radius of the fuel channels in the outer zone is modified to be larger than the radius of the fuel channels in the inner zone to improve the breeding ratio [6, 5].

20 Basically, the MSR has been designed to apply the Th/ $^{233}\text{U}$  fuel cycle [7, 6, 8, 3]. Hence, the fertile isotope  $^{232}\text{Th}$  is converted to the fissile isotope  $^{233}\text{U}$ , an isotope that is not exist in nature. Therefore it is required to examine available fissile materials (e.g.,  $^{235}\text{U}$  and Pu) to replace the  $^{233}\text{U}$  in the startup

fuel [9, 10]. The thorium fuel cycle transition can be achieved after reaching the  
25 doubling time<sup>1</sup> of  $^{233}\text{U}$ .

Betzler, et al. discussed the simulation of the start-up of a MSBR unit cell  
with LEU (19.79%) and Pu from Light Water Reactor (LWR) spent fuel (SF) as  
initial fissile materials [9]. They concluded that the plutonium vector extracted  
from LWR SF serves as the best alternative source to  $^{233}\text{U}$  thanks to the highest  
30 ratio of fissile isotopes [9]. Zou, et al. introduced two approaches for the thorium  
fuel cycle transition in Thorium-based Molten Salt Reactor (TMSR): in-core  
transition and ex-core transition. In the former way, the TMSR is launched with  
existing fissile material and thorium as a fertile material, then the bred  $^{233}\text{U}$   
from thorium is rerouted into the core for criticality. In contrast, the latter way  
35 tends to store the bred  $^{233}\text{U}$  out of the core until there is enough amount to start  
a new TMSR [10]. Meanwhile, Zou, et al. studied the transitioning to thorium  
fuel cycle in a small modular Th-based molten salt reactor (smTMSR) using  
TRUs as startup fuel. They concluded that the transition to thorium fuel cycle  
can be achieved in thermal smTMSR with a proper fuel fraction [11]. Heuer,  
40 et al., discussed the transition characteristics of the Molten Salt Fast Reactor  
(MSFR) under different launching scenarios (e.g., enriched uranium and TRU)  
[12].

Indeed, there are various researches that revolve around starting the MSRs  
with fissile materials alternative to  $^{233}\text{U}$ . Many of these researches focus on the  
45 fast-spectrum MSRs [13, 14, 12, 15], while little focus on thermal-spectrum MSRs  
[9, 11, 10]. Nevertheless, starting the Single-fluid Double-zone Thorium-based  
Molten Salt Reactor (SD-TMSR) with other fissile materials (except  $^{233}\text{U}$ ) not  
found in the literature. Therefore, the main object of the present paper is to  
discuss the simulation of the operation of SD-TMSR for a long period of time  
50 (60 years) with different initial fissile materials and without any external feed of  
 $^{233}\text{U}$  to achieve the thorium fuel cycle transition. To do that, we investigate five  
types of initial fissile materials based on Low-enriched uranium (LEU), Pu, and

---

<sup>1</sup>Time required to produce enough amount of  $^{233}\text{U}$  to trigger a new SD-TMSR.

Transuranic elements (TRU) from LWR SF [16]. Moreover, two different feed mechanisms are used as follows:

- 55 • Continuous feed flow of thorium and  $^{233}\text{U}$  from **Pa-decay tank**, where the removal rate of  $^{233}\text{Pa}$  = feed rate of  $^{233}\text{U}$ . [9].
- Continuous feed flow of (Heavy Metal (HM) except for Th) + all or part of  $^{233}\text{U}$  from **Pa-decay tank**.

This present paper is organized as follows: after an introduction about MSR systems, the model description is discussed in section 2. Methodology and tools is descried in section 3. Extraction and feed mechanisms are addressed in section 4. Section 5 focuses on the results and discussion. Finally, section 6 highlights the conclusions.

## 2. Model description

### 65 2.1. Geometry

The SD-TMSR design model was introduced by the CAS during the strategic project “Future Advanced Nuclear Energy – Thorium-based Molten Salt Reactor System (TMSR)” in 2011 [5, 17, 18, 19]. The design of SD-TMSR is inspired by Molten Salt Breeder Reactor (MSBR) [20] after some modification in the geometry to control the positive temperature coefficient in MSBR. The SD-TMSR model is described deeply in [5]. Figure 1 illustrates the quarter-core model configuration of the SD-TMSR. The active zone is a right cylinder with height and diameter equal to 460 cm. Assemblies of graphite<sup>2</sup> hexagonal prisms fill the core. The side length of the graphite hexagonal prism was optimized in [5] and found to be 7.5 cm. The liquid fuel circulates continuously through the fuel channels that pierces the graphite hexagonal prisms. The active zone is divided into two different zones to enhance Th-U breeding performance. The

---

<sup>2</sup>We choose graphite density of  $2.3 \text{ g/cm}^3$ , to validate our results against results in the literature [5, 6].

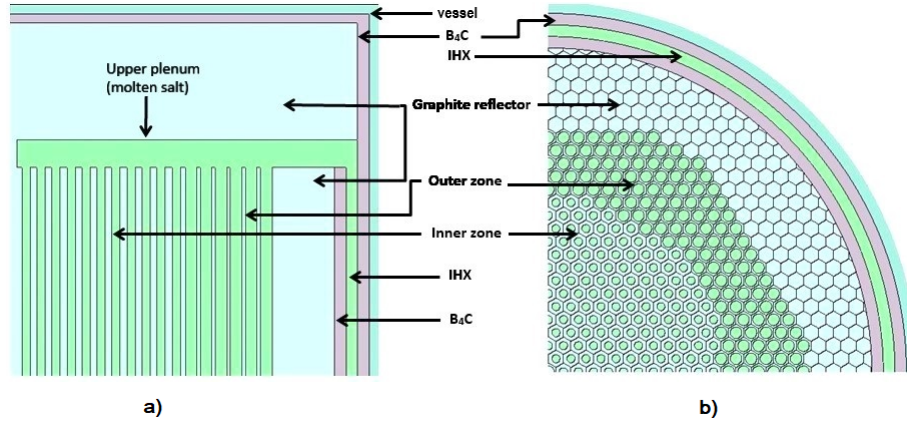


Figure 1: The quarter-core model configuration of the SD-TMSR a) Longitudinal view b) Cross-sectional view at the horizontal midplane.

radius of the fuel tubes in the outer zone is 5 cm and the radius of the fuel tubes in the inner zone is 3.5 cm. Moreover, axial and radial reflectors from graphite surround the active zone to maximize neutron flux. The core is surrounded by B<sub>4</sub>C cylinder that acts as a shield against heat and neutrons radiation. Another Ni-based (hastelloy N) cylinder surrounds the whole core and provides structure and heat protection. The main characteristics of the SD-TMSR are listed in Table 1.

## 2.2. Fuel composition

The general composition of the liquid fuel salt in this work is 70LiF - 17.5BeF<sub>2</sub> - 12.5(HM)F<sub>4</sub> mole%, where HM is the heavy metal (i.e. thorium + different fissile materials). As previously mentioned, the aim of this paper is to simulate the operation of SD-TMSR for a long period of time (60 years) with different initial fissile materials and without any external feed of <sup>233</sup>U. Therefore, five different types of initial fissile materials based on LEU, Pu, and TRU from LWR SF are investigated as follows:

- (1) low-enriched uranium (LEU) (19.79%);
- (2) Pu mixed with LEU (19.79%);
- (3) Pu reactor-grade [21];

Table 1: The main characteristics of the SD-TMSR [5]

Thermal power, $MW_{th}$	2,250
Fuel salt components	$LiF-BeF_2-(HM)F_4$
Fuel composition, mole%	70-17.5-12.5
$^7Li$ enrichment, %	99.995
Fuel temperature, K	900
Fuel density at 900 K, $g/cm^3$	3.3
Fuel dilatation coefficient, $g/(cm^3 \cdot K)$	$-6.7 \times 10^{-4}$
Graphite density, $g/cm^3$	2.3
$B_4C$ density, $g/cm^3$	2.52
$^{10}B$ enrichment, %	18.4
Core diameter, cm	460
Core height, cm	460
Side length of the graphite hexagonal prism, cm	7.5
Inner radius, cm	3.5
Outer radius, cm	5
Ratio of molten salt and graphite in the inner zone	0.357
Ratio of molten salt and graphite in the outer zone	1.162
Fuel volume, $m^3$	52.9

Table 2: Reactor-grade plutonium vector [21]

$^{238}\text{Pu}$	$^{239}\text{Pu}$	$^{240}\text{Pu}$	$^{241}\text{Pu}$	$^{242}\text{Pu}$
1.3	60.3	24.3	9.1	5

Table 3: TRU vector (%) [16]

$^{237}\text{Np}$	$^{238}\text{Pu}$	$^{239}\text{Pu}$	$^{240}\text{Pu}$	$^{241}\text{Pu}$	$^{242}\text{Pu}$	$^{241}\text{Am}$	$^{243}\text{Am}$	$^{244}\text{Cm}$	$^{245}\text{Cm}$
6.3	2.7	45.9	21.5	10.7	6.7	3.4	1.9	0.8	0.1

(4) transuranic (TRU) elements from LWR SF [16];

(5) and  $^{233}\text{U}$  for comparison purpose.

The reactor-grade plutonium and TRU vector (%) are summarized in Table 2 and 3, respectively.

The isotopic compositions of plutonium recovered from the spent fuel composition of commercial LEU Pressurized Water Reactor (PWR) that has released 33  $\text{GWd/t}$  fission energy and has been cooled for 10 *years* before reprocessing [22, 21]. As well, the isotopic compositions of TRU have been taken from the SF of UOX PWR (after one use and without multi-recycling) with 60  $\text{GWd/t}$  burnup, and after 5 *years* cooling [16]. The molar composition of startup fuel for all five cases is listed in Table 4. Meanwhile, the corresponding initial nuclei inventories with different types of fuel are tabulated in Table 5.

### 3. Methodology and tools

Simulation of Liquid-fueled Molten Salt Reactor (MSR) systems requires computational software that must support online fuel salt reprocessing and refueling [23]. In this work, SERPENT-2 version 2.1.31 beta<sup>3</sup> [24] is used to simulate the full-core of the SD-TMSR with different types of initial fuel. The

<sup>3</sup>SERPENT-2 is a Three Dimensions (3D) continuous energy Monte Carlo neutron transport and burn-up code.

Table 4: Composition of startup fuel mole%

Molecule	LEU (19.79%)	Pu mixed with en- riched U (19.79 wt-%)	Pu reactor- grade	TRU	<sup>233</sup> U
LiF	70	70	70	70	70
BeF <sub>2</sub>	17.5	17.5	17.5	17.5	17.5
ThF <sub>4</sub>	8.25	7.5	10.75	8.65	12.3
UF <sub>4</sub>	4.25	4.75			0.2
PuF <sub>3</sub>		0.25	1.75		
TRUF <sub>3</sub>				3.85	

extension of SERPENT code accounts for continuous online reprocessing and  
115 refueling [25]. Meanwhile, ENDF-VII.0 cross-section library is adopted for all  
calculations. The results demonstrate full-core runs of  $12.5E+06$  neutron history  
per depletion step. The full burnup time of the SD-TMSR was 60 years with  
statistical error in  $k_{eff}$  equal to  $\pm 36 pcm$ . The online extraction of Fission  
Products (FPs) and noble gases provides many benefits for MSRs. For example,  
120 it would reduce the fissile inventory required to achieve criticality and improve  
the breeding ratio. Figure 2 shows a flow chart of the calculation steps.

As shown in Figure 2, after launched the input file, an advanced matrix  
exponential solution based on the Chebyshev Rational Approximation Method  
(CRAM) [26] used to solve the Bateman equation. Then, the system extracted  
125 gaseous FPs and other materials (non-dissolved metals, lanthanides, and soluble  
metals except Pu) in a proper time. This can be done by set the flow rate of  
gaseous FPs and other materials from the fuel to the **FP-waste tank**<sup>4</sup>. Specif-

<sup>4</sup>An imaginary tank used to store the gaseous FPs and the other materials (non-dissolved metals, lanthanides, and soluble metals except protactinium).



Table 5: Initial nuclei inventories (in grams) of the SD-TMSR with different types of fuel.

Molecule	LEU (19.79%)	Pu mixed with en- riched U (19.79%)	Pu reactor- grade	TRU	$^{233}\text{U}$
$^{232}\text{Th}$	6.24E+07	4.67E+07	6.75E+07	5.44E+07	7.69E+07
$^{233}\text{U}$					1.30E+06
$^{235}\text{U}$	3.17E+06	6.01E+06			
$^{238}\text{U}$	1.28E+07	2.43E+07			
$^{237}\text{Np}$				1.58E+06	
$^{238}\text{Pu}$		1.60E+04	1.13E+05	6.78E+05	
$^{239}\text{Pu}$		9.59E+05	6.76E+06	1.15E+07	
$^{240}\text{Pu}$		3.99E+05	2.82E+06	5.40E+06	
$^{241}\text{Pu}$		1.60E+05	1.13E+06	2.69E+06	
$^{242}\text{Pu}$		6.39E+04	4.51E+05	1.68E+06	
$^{241}\text{Am}$				8.53E+05	
$^{242}\text{Am}$					
$^{243}\text{Am}$				4.77E+05	
$^{244}\text{Cm}$				2.01E+05	
$^{245}\text{Cm}$				2.51E+04	
Total mass of HM without $^{232}\text{Th}$	1.60E+07	3.20E+07	1.13E+07	2.51E+07	1.30E+06

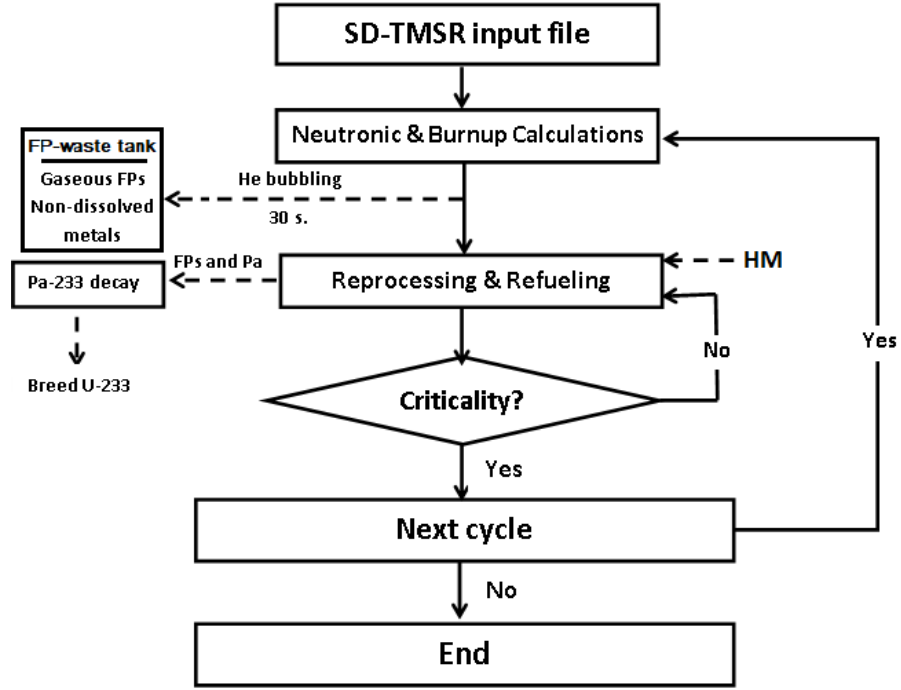


Figure 2: Flow chart of the calculation procedures.

ically, protactinium was removed from the fuel with a certain flow rate into the external tank, **pa-decay tank**<sup>5</sup>, to decay and produce  $^{233}\text{U}$ <sup>6</sup>. The produced  $^{233}\text{U}$  is used as a fresh fissile fuel and the residual  $^{233}\text{U}$  is the net production of  $^{233}\text{U}$ . The MSR burnup routine provided by SERPENT-2 allows changes the flow rates (*mflow*) of the isotopes during reactor operation [25]. The mass of the fissile and fertile materials needed to achieve criticality is calculated at the end of the cycle. Then, this mass is added to the core at the beginning of the cycle by a certain flow rate.

<sup>5</sup>An imaginary tank used to store protactinium extracted from the core.

<sup>6</sup>The  $^{233}\text{Pa}$  is removed and left to decay into  $^{233}\text{U}$  with  $\tau_{1/2} \approx 27\text{ d}$ .

#### 4. Feed and extraction rates

In the present work, two different feed mechanisms are used. The first mechanism allows continuous feed flow of thorium and  $^{233}\text{U}$  from **pa-decay tank**. In contrast, the second mechanism adopts continuous feed flow of (Heavy Metal (HM) except for Th) + all or part of  $^{233}\text{U}$  from **Pa-decay tank**.  
 140 The fission products act as poisons in the MSRs; they negatively impacting the reactivity. Therefore, FPs must be extracted during reactor operation. Consider  $T_r$  as the time during which the total fuel salt is reprocessed and  $dN_e$  as the amount of particular element  $e$  with inventory  $N_e$  that the MSR extracts during  
 145 time  $dt$ ; thus [6]

$$\frac{dN_e}{dt} = N_e \frac{\varepsilon_e}{T_r}, \quad (1)$$

where  $\varepsilon_e$  is the removal efficiency. Equation 1 gives the removal constant  $\lambda_e$  [ $s^{-1}$ ] (the rate at which the material is removed), where  $\lambda_e = \varepsilon_e/T_r$ . The removal constant  $\lambda_e$  of gaseous and other fission products is precisely calculated and summarized in Table 6. The effective reprocessing time for the gaseous  
 150 FPs and non-dissolved metals was set to 30 seconds (removal constant  $\lambda_e = -0.0333 s^{-1}$ ), because such elements must be extract promptly and continuously via He bubbling system. In contrast, extracting the soluble FPs, lanthanides, and protactinium can be done by the chemical reprocessing (i.e. fluorination and reduction reaction). Therefore, the system reprocesses a specific amount  
 155 of fuel salt daily. In the present work, the effective extraction time for soluble FPs is  $\approx 10.59$  days ( $\lambda_e = -1.092 \times 10^{-6} s^{-1}$ ), which is equivalent to  $5 \text{ m}^3/\text{d}$  of chemical reprocessing rate [6, 5]. The effective feed rates of the heavy metals (HM) are changed during reactor operation to conserve the total fuel mass and criticality.

Table 6: The reprocessing table.

Reprocessing group	Element	Reprocessing time	Removal constant $\lambda_e$ [ $s^{-1}$ ]
Gaseous FPs and non-dissolved metals	H, He, N, O, Ne, Ar, Kr, Nb, Mo, Tc, Ru, Rh, Pd, Ag, Sb, Te, Xe, Lu, Hf, Ta, W, Re, Os, Ir, Pt, Au and Rn.	30s	-3.333E-02
Lanthanides and other soluble FPs	Zn, Ga, Ge, As, Se, Br, Rb, Sr, Y, Zr, Cd, In, Sn, I, Cs, Ba, La, Ce, Pr, Nd, Pm, Sm, Eu, Gd, Tb, Dy, Ho, Er, Tm and Yb.	10.599 d (5 m <sup>3</sup> /d)	-1.092E-06
Protactinium	Pa	10.599 d (5 m <sup>3</sup> /d)	-1.092E-06

## 160 5. Results and discussion

### 5.1. Thorium feed mechanism

The first mechanism adopts continuous feed flow of external thorium and <sup>233</sup>U from Pa-decay tank. Hereinafter the first mechanism will be mentioned as the thorium feed mechanism. The molar fraction of the heavy metal in the initial fuel was kept constant and equal to 12.5 mole% for all cases. Besides, the initial fissile material fraction was increased for the five fuel salt compositions until the SD-TMS reactor was sufficiently critical at the Beginning Of Life (BOL). Figure 3 illustrates the change of the effective multiplication with Effective Full-Power Years (EFPY) for the thorium feed mechanism. As shown in Figure 3, the effective multiplication factor ( $k_{eff}$ ) decreases sharply during the first 25 years of reactor operation for the first four cases.  $k_{eff}$  decreases as a result of depletion of the initial fissile materials and generation of the neutron poisons (FPs). Thus, the reactor becomes subcritical within a relatively short time ( $\approx 4$  years in the

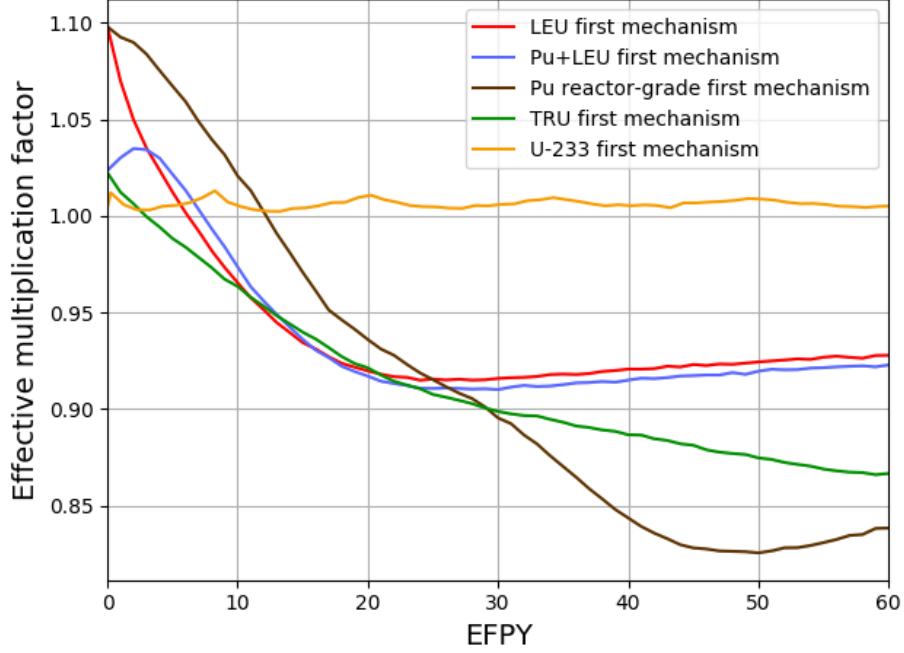


Figure 3: The change of the effective multiplication factor during 60 EFPY of reactor operation for thorium feed mechanism (confidence interval  $\pm\sigma$  is shaded).

TRU case and  $\approx 12$  years in the Pu reactor-grade case). The amount of  $^{233}\text{U}$  generated in the SD-TMSR is not enough to conserve the reactor criticality and overcome the neutron absorption in the initial fertile isotopes. Nevertheless, the continuous feed flow of thorium and  $^{233}\text{U}$  helps to operate the SD-TMSR for a long period of time (the U-233 case). Additionally, the initial molar fraction in the LEU and Pu reactor-grade cases was increased more (see Figure 3) to counteract the absorption of neutrons in the non-fissile heavy metals added with the initial fuel salt. But  $k_{eff}$  still decreases below 1.0, as a result of increasing the non-fissile heavy metals in the initial fuel [9].

### 5.2. Non-thorium feed mechanism

The second mechanism allows continuous feed flow of  $^{233}\text{U}$  from Pa-decay tank and Heavy Metal except for Th. Hereinafter the second mechanism will

be mentioned as the non-thorium feed mechanism. Figure 4 shows the change of the effective multiplication during 60 EFPY of reactor operation for the non-thorium feed mechanism. As shown in Figure 4, the SD-TMS reactor was sufficiently critical at the Beginning Of Life (BOL). Both Pu reactor-grade and TRU case show promising results relative to the other two cases (i.e. LEU and Pu+LEU). For the Pu reactor-grade fuel salt, the amount of  $^{233}\text{U}$  generated in the SD-TMSR in addition to the external feed flow of Pu are sufficient to maintain the reactor criticality and overcome the neutron absorption in the initial non-fissile isotopes. This may be attributed to the fact that the spectrum in the Pu reactor-grade initial core is hardened that is more thorium is being converted to  $^{233}\text{U}$ . For the TRU fuel salt, the amount of  $^{233}\text{U}$  and the external feed flow of TRU is barely enough to operate the reactor for a long period of time ( $\approx 40$  years) without any external feed of  $^{233}\text{U}$ . Nevertheless,  $k_{eff}$  decreases with the burnup because the Minor Actinides<sup>7</sup> (MA) accumulating in the core as a result of continuous TRU feed. As shown in Figure 4, the LEU and Pu+LEU fuel are less attractive for non-thorium feed mechanism. The continuous LEU feed increases the amount of fertile  $^{238}\text{U}$  and consequently, reduces the feasibility of such fissile materials. The continuous feed of  $^{233}\text{U}$  without  $^{232}\text{Th}$  will lead to supercritical reactor, thus the  $^{233}\text{U}$  case is excluded from non-thorium feed mechanism.

According to the  $k_{eff}$  results, Pu reactor-grade and TRU fissile materials are selected and discussed in the following.

### 5.3. Pu reactor-grade, TRU, and $^{233}\text{U}$ initial fuel

In this section, the simulation of the SD-TMSR with Pu reactor-grade and TRU fissile materials is discussed. Besides, the  $^{233}\text{U}$  case is listed for comparison. Figure 5 demonstrates the dynamics of heavy metal refill rate during 60 EFPY of SD-TMSR operation. The heavy metal refill rate was adjusted to maintain;

---

<sup>7</sup>In the present work, the Minor Actinides (MA) include Np, Am and Cm.

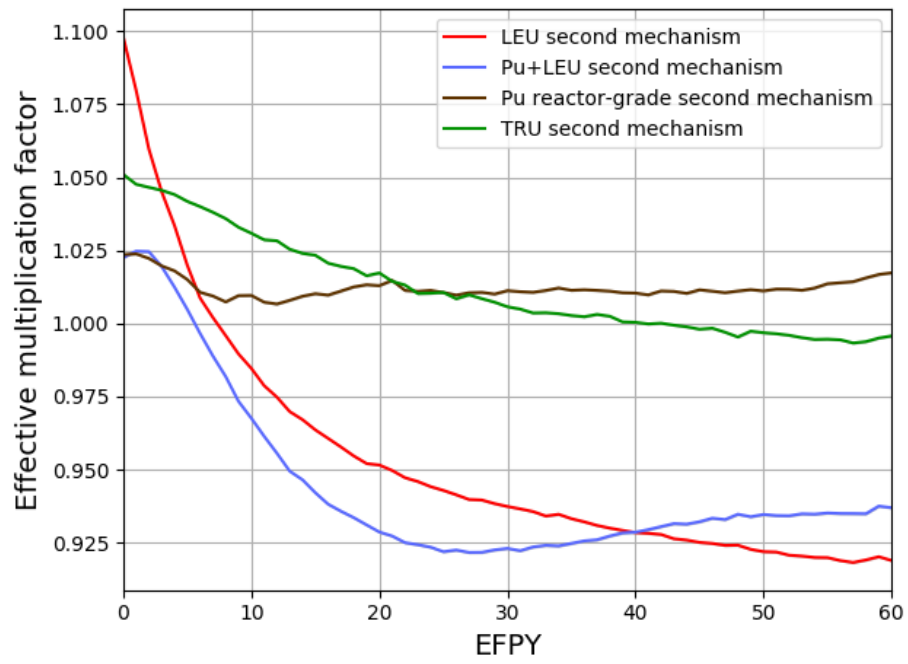


Figure 4: The change of the effective multiplication factor during 60 EFPY of reactor operation for non-thorium feed mechanism (confidence interval  $\pm\sigma$  is shaded).

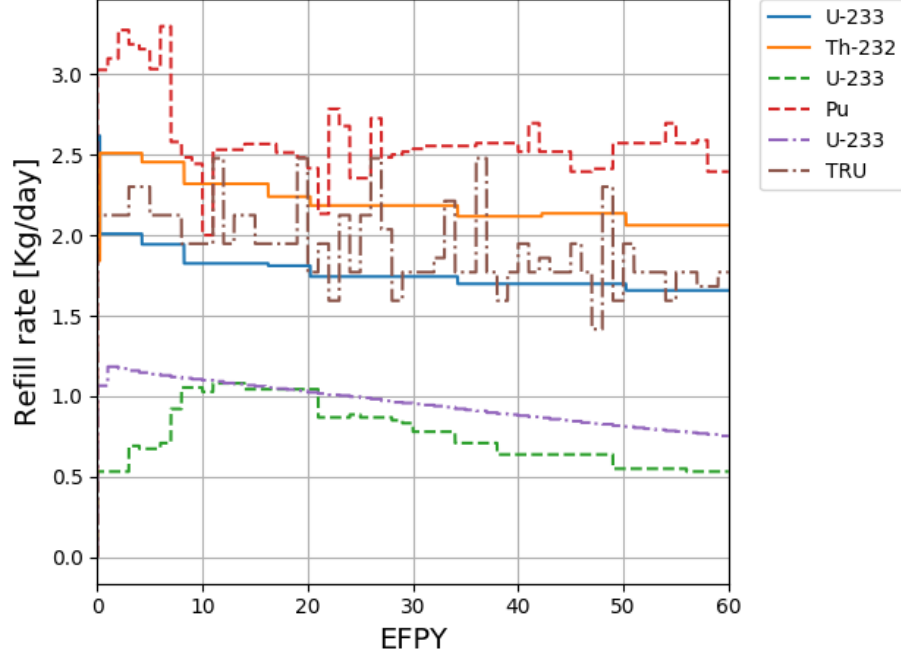


Figure 5: Dynamics of heavy metal refill rate during 60 EFPY of reactor operation. Solid lines for  $^{233}\text{U}$  case, dashed lines for Pu reactor-grade case, and dotted lines for TRU case.

the reactor criticality and total fuel mass almost constant<sup>8</sup> during the reactor operation. In  $^{233}\text{U}$  case, the mean values of  $^{233}\text{U}$  and  $^{232}\text{Th}$  refill rate are 1.77  
 215 and 2.21  $\text{kg/d}$ , respectively. As well, in the Pu reactor-grade case, the mean values of  $^{233}\text{U}$  and Pu refill rate are 0.75 and 2.75  $\text{kg/d}$ , respectively. In the TRU case, the mean values of  $^{233}\text{U}$  and TRU refill rate are 0.90 and 2.0  $\text{kg/d}$ , respectively.

Figure 6 and 7 describe the evolution of important isotopes for  $^{233}\text{U}$ , Pu and  
 220 TRU cases respectively. From Figure 6, the mass of Pa in the fuel salt is almost constant and reaches 17.8  $\text{kg}$  at the end of the operation time. In addition, the mass of Minor Actinides (MA) increases with time; however, by applying online reprocessing, its value remains relatively low. As well, the total mass of Pu

<sup>8</sup>The variation of the total fuel mass is less than 0.1%



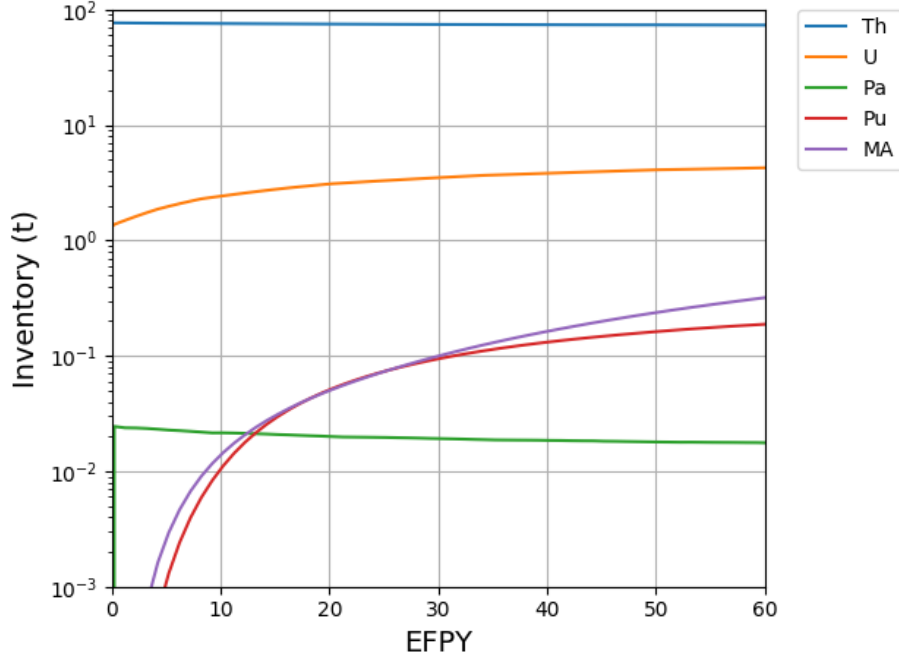


Figure 6: Evolution of the important nuclides inventories for  $^{233}\text{U}$  case (MA involves Np, Am, Cm).

increases with burnup. The level of Pu in the fuel correlates with the mass of the MA, and Pu. MA need more time to reach equilibrium. The total mass of U increases with burnup and reaches equilibrium after  $\approx 27$  years. As shown in Figure 6, refueling the core with Th helps maintain an almost constant inventory throughout the full operation time.

The Pa extraction time was adjusted to be 30 seconds for Pu and TRU cases to avoid poisoning the core. Therefore, Figure 7 shows that the mass of Pa in the fuel for Pu and TRU cases is relatively low when compared to the  $^{233}\text{U}$  case. Major isotopes for the three cases reaches the equilibrium state after  $\approx 30$  years (see Figure 6 and 7).

Figure 8 illustrates the variation of thorium mass in the fuel salt for  $^{233}\text{U}$ , Pu reactor-grade and TRU cases, respectively. In  $^{233}\text{U}$  case, we apply the thorium feed mechanism, thus thorium mass decreases by only 3.2 % at the end of

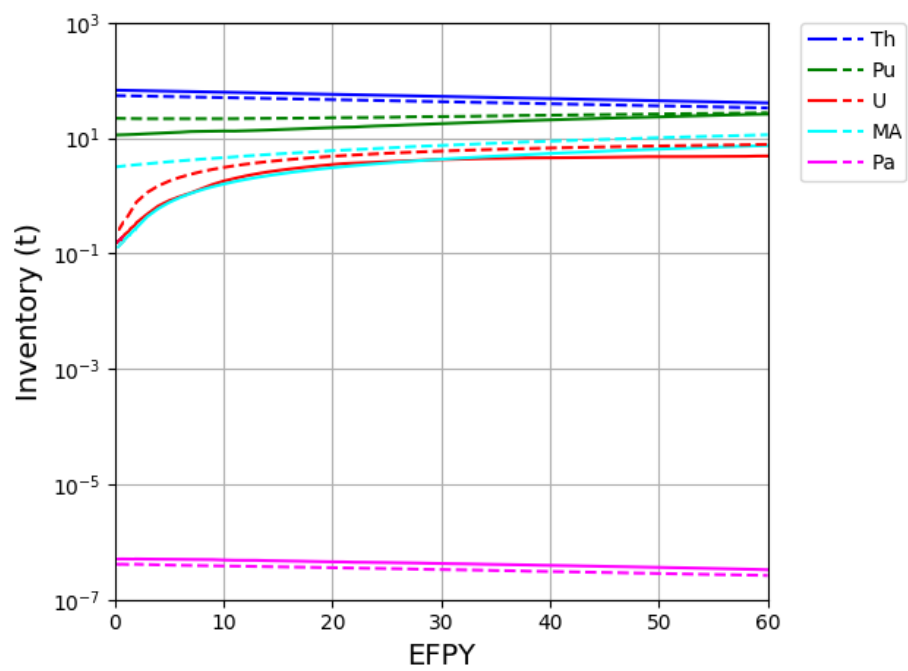


Figure 7: Evolution of the important nuclides inventories for Pu reactor-grade case (solid lines) and for TRU case (dashed lines).

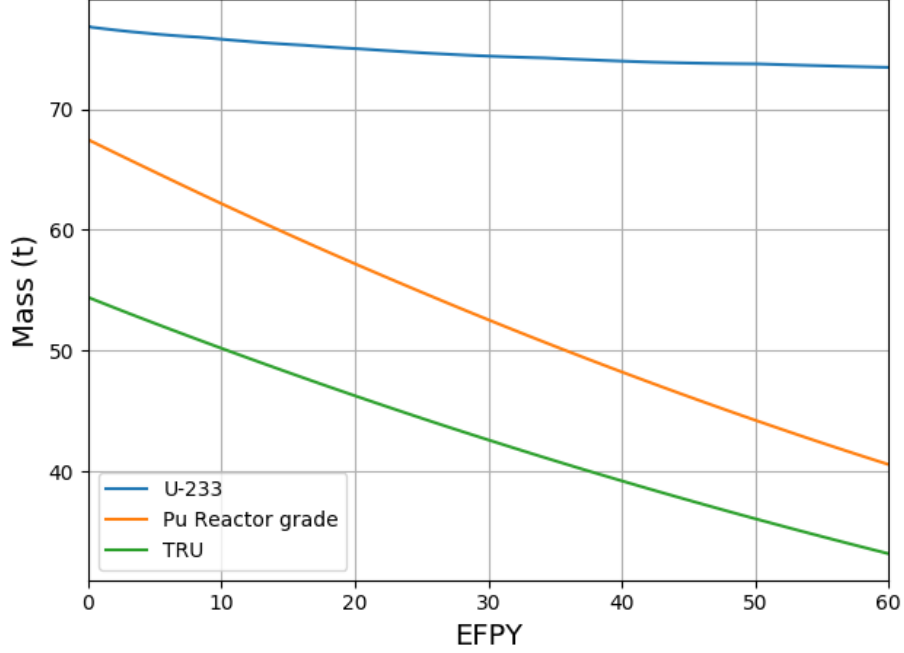


Figure 8: The variation of thorium mass in the fuel salt for  $^{233}\text{U}$ , Pu reactor-grade and TRU cases, respectively.

operation time (60 years). In contrast, thorium mass decreases significantly in Pu and TRU cases according to the non-thorium feed mechanism. Thorium mass decreases by 39.2 % and 37.96 % in Pu reactor-grade and TRU cases, respectively. The more decreasing in thorium mass, the more effective utilization of thorium fuel cycle. Consequently, the Pu reactor-grade initial fuel may help to utilize thorium fuel cycle more effective.

Figure 9 demonstrates the mass of  $^{233}\text{U}$  in the fuel salt for  $^{233}\text{U}$ , Pu reactor-grade and TRU cases, respectively. One can see that the mass of the  $^{233}\text{U}$  reaches the equilibrium state after  $\approx 30$  years. Meanwhile, the amount of  $^{233}\text{U}$  is sufficient to maintain criticality in the three cases.

In the non-thorium feed mechanism, the SD-TMSR is continuously refueled for criticality, which increases the Pu proportion in the molten salt. According to the literature, the limit of Pu solubility in the FLiBe salt is  $\approx 4.0$  % [27, 28].

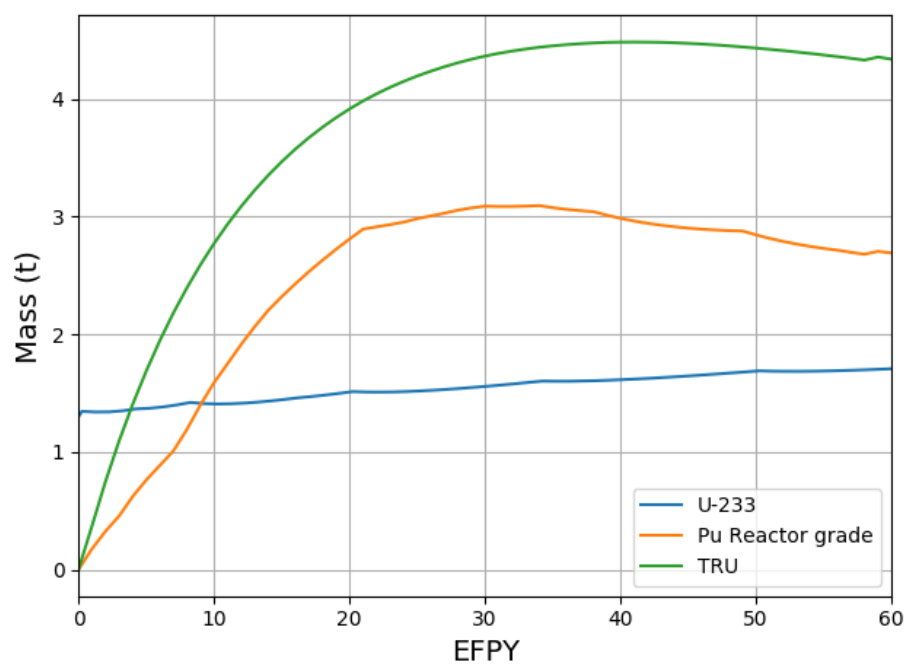


Figure 9: Mass of  $^{233}\text{U}$  in the fuel salt for  $^{233}\text{U}$ , Pu reactor-grade and TRU case, respectively.

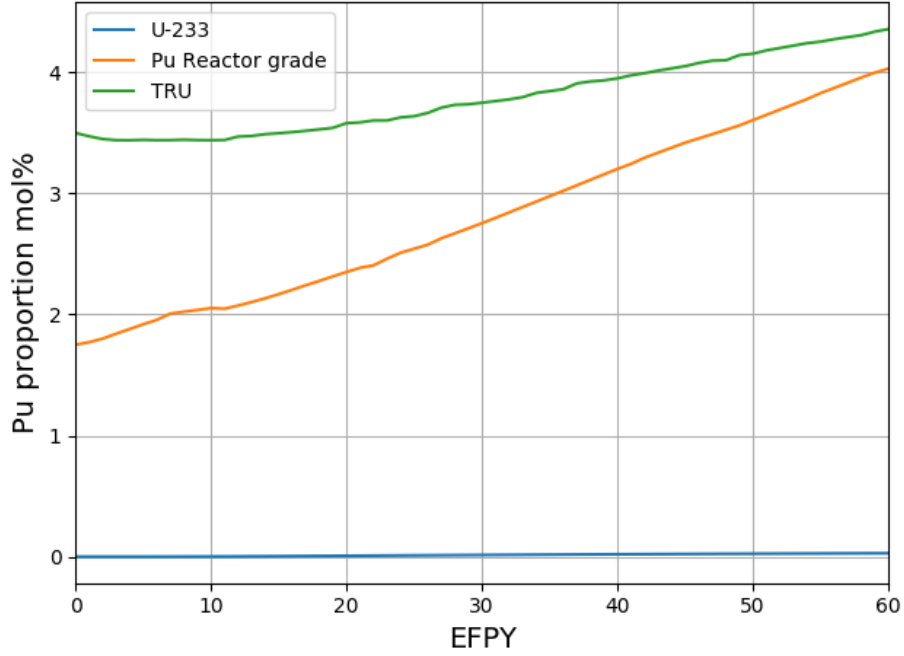


Figure 10: The Pu proportion in the fuel salt (mole%).

Figure 10 represents the Pu proportion in the fuel salt (mole%). In  $^{233}\text{U}$  and Pu reactor-grade cases, the Pu proportion increases slightly but still below its solubility limit. On the other hand, the Pu proportion in the molten salt loaded by TRU increases with operation time and reaches the Pu solubility limit after  $\approx 40$  years. This issue may be solved by increasing the reactor operation temperature and or reducing the HM initial inventory [10].

Figure 11 demonstrates the net production of  $^{233}\text{U}$  as a function of burnup. In TRU case, the net production of  $^{233}\text{U}$  is almost zero, nevertheless, the reactor becomes subcritical after 40 years of operation. In  $^{233}\text{U}$  and Pu reactor-grade cases, the net production of  $^{233}\text{U}$  increases with burnup and reaches about 1.77 t and 10 t, respectively at the end of operation lifetime. It worth noting that thorium feed mechanism is applied in  $^{233}\text{U}$  case, while, non-thorium feed mechanism is adopted in Pu reactor-grade cases. As shown in Figure 11, after 26 years the net production of  $^{233}\text{U}$  reaches 1.3 t; this is sufficient to start-up another

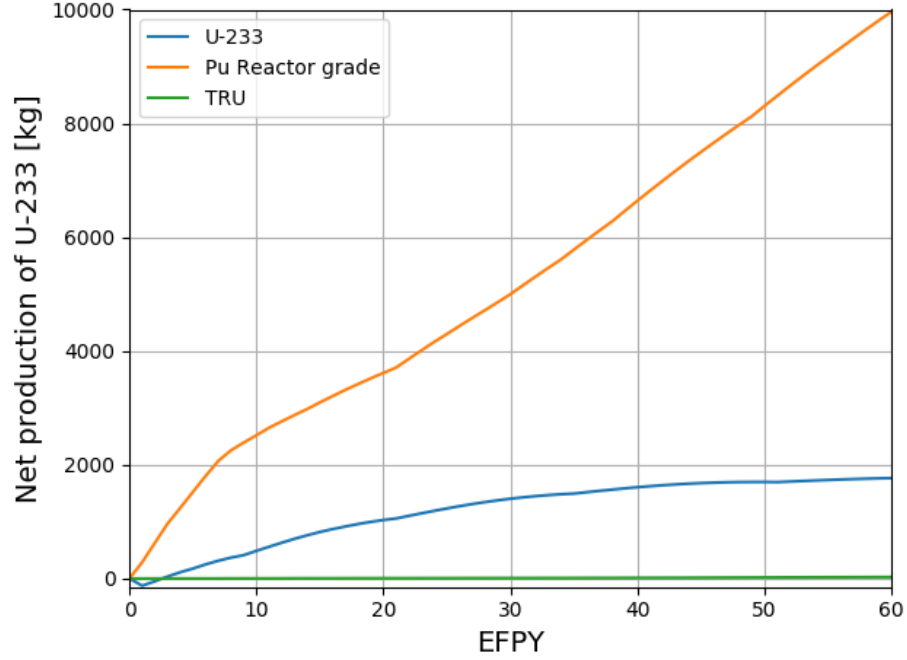


Figure 11: Net production of  $^{233}\text{U}$  during burn-up period (60 EFY).

SD-TMSR. Similarly, one can see that the same amount of  $^{233}\text{U}$  (i.e. 1.3 t) can  
 265 be achieved after  $\approx 4.5$  years if we applied the non-thorium feed mechanism  
 on the SD-TMSR that initially loaded by Pu reactor-grade alternative to  $^{233}\text{U}$ .  
 In addition, Figure 11 also shows that the net production of  $^{233}\text{U}$  during the  
 first 455 days is negative, thus about 175.28 kg of  $^{233}\text{U}$  must be added during  
 this period. In conclusion, the thorium fuel cycle transition can be achieved by  
 270 selecting the proper feed mechanism and initial fissile material.

#### 5.4. Neutron spectrum

Figure 12 represents the neutron flux per unit lethargy for full-core SD-TMSR  
 model in the energy range from  $10^{-8}$  to 10 MeV for the  $^{233}\text{U}$ , Pu reactor-grade,  
 and TRU started case. In  $^{233}\text{U}$  case, at the EOL, the neutron spectrum is  
 275 harder than at BOL due to the accumulation of the Pu and other strong thermal  
 neutron absorbers in the fuel salt. For Pu reactor-grade and TRU cases, during

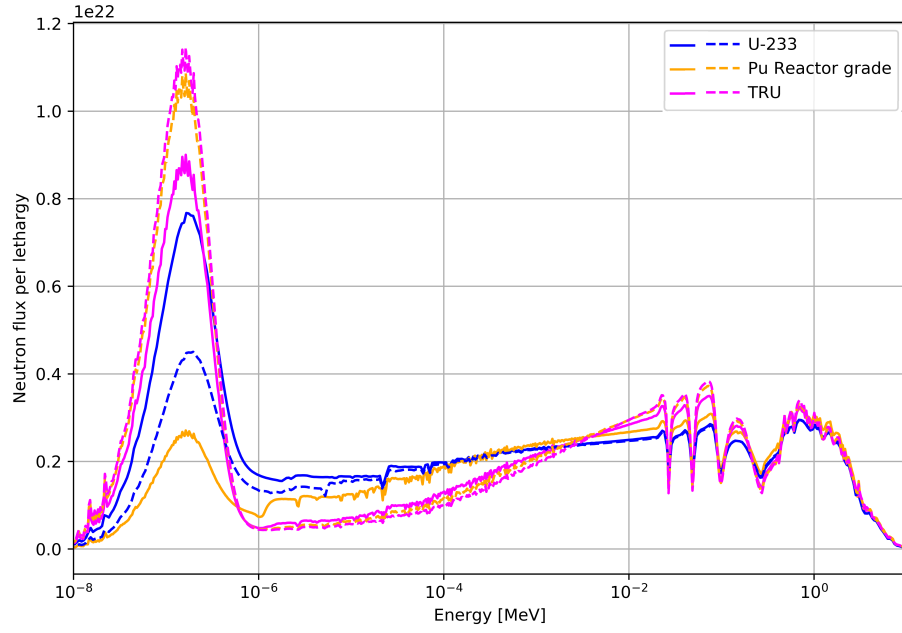


Figure 12: The neutron flux energy spectrum at BOL (solid lines) and EOL (dashed lines) for  $^{233}\text{U}$ , Pu reactor-grade, and TRU case.

the reactor operation, the fissile Pu is depleted and the  $^{233}\text{U}$  becomes the major fissile isotope (see Figure 9), the neutron spectrum softens and becomes similar to a thermal spectrum of the TMSR.

280 The comparison between the two feed mechanisms with different types of initial fuel is listed in Table 7.

Table 7: Comparison between the two feed mechanisms for the five different types of initial fuel.

Feed mechanism	Initial fuel	LEU	Pu	Pu	TRU	$^{233}\text{U}$
		(19.79%)	mixed with enriched U (19.79 wt-%)	reactor-grade		
Thorium feed mechanism		Not work	Not work	Not work	Not work	Work
Non-thorium feed mechanism		Not work	Not work	Work well with positive net production of $^{233}\text{U}$	Work for 40 <i>years</i> with net production of $^{233}\text{U}$ = zero	Not examined (super-critical reactor)



### 5.5. Neutron flux

Figures 13, 14 show the radial distribution of fast (energy range between 0.625 eV and 20 MeV) and thermal (energy range between  $10^{-5}$  eV and 0.625 eV) neutron flux for three different initial fissile materials in the fuel salt ( $^{233}\text{U}$ , reactor-grade plutonium, TRU) at startup and at equilibrium (after  $\approx 30$  years of operation). Actinides evolution and poisonous fission products accumulation for various initial fissile compositions demonstrated different effect on the SD-TMSR neutronics performance. For the Th/ $^{233}\text{U}$ , thermal neutron flux is suppressed at the equilibrium state because fissile  $^{233}\text{U}$  in the core is being substituted with heavier fissile actinides:  $^{235}\text{U}$ ,  $^{239}\text{Pu}$ , and  $^{241}\text{Pu}$  which is in a good agreement with results the literature [7, 29].

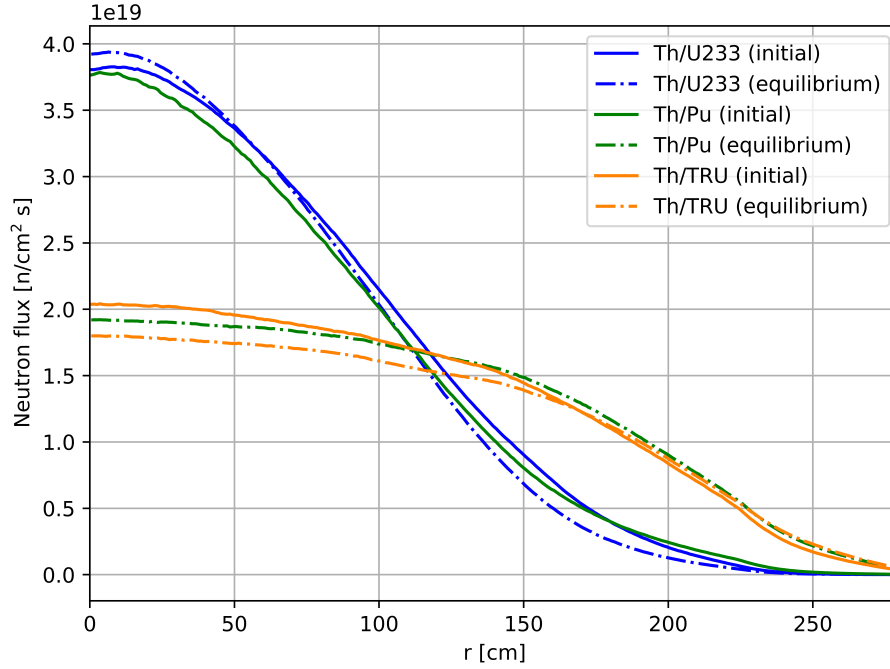


Figure 13: Radial fast neutron flux distribution for 3 different initial fuel salt compositions at startup and equilibrium (the fast flux confidence interval  $\pm\sigma < 2.5\%$  for all cases).

Opposite observation has been made for reactor-grade Pu and TRU cases. For these cases, thermal neutron flux is increasing during operation while fast neutron

295 flux is decreasing. The fissile Pu (generates relatively hard spectrum) from initial fuel salt composition is gradually substituted with the  $^{233}\text{U}$  (generates relatively soft spectrum), produced from the fertile  $^{232}\text{Th}$ . During reactor operation, the  $^{233}\text{U}$  becomes primary fissile isotope which leads to the neutron spectrum softening of the reactor.

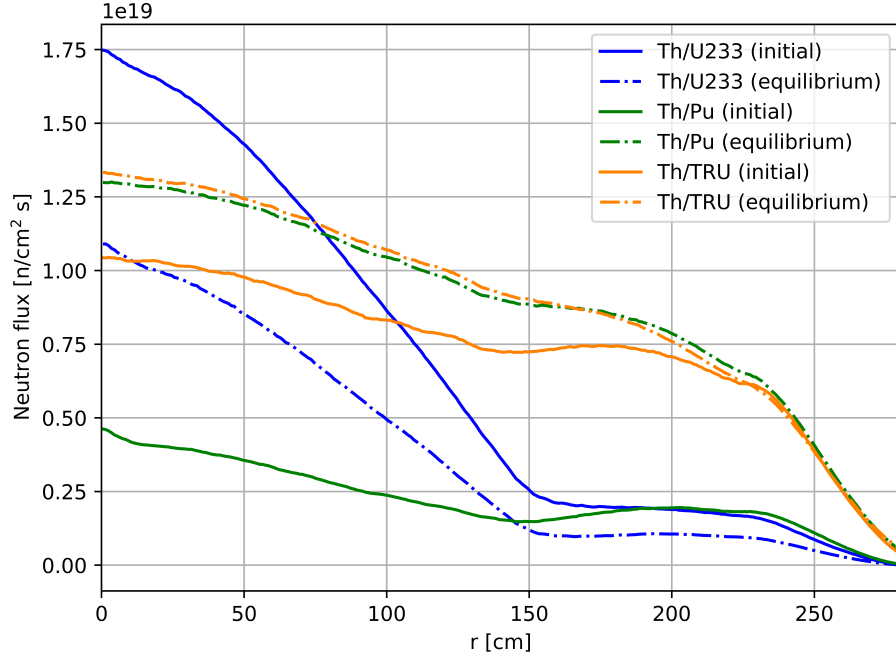


Figure 14: Radial thermal neutron flux distribution for 3 different initial fuel salt compositions at startup and equilibrium for initial and equilibrium fuel salt composition (the thermal flux confidence interval  $\pm\sigma < 1.6\%$  for all cases).

300 Notably, more changes in thermal neutron flux shape and magnitude for  $^{233}\text{U}$  case were observed in the inner core zone ( $R \lesssim 150$ ) than in the outer core zone. In contrast, for Pu reactor-grade and TRU case, large changes were observed for thermal neutron flux in the outer core zone and reflector. Additionally, Figure 14 shows relatively large changes in thermal flux leakage from the core for Pu case. 305 Overall, the SD-TMSR core design was optimized for  $^{233}\text{U}$  fissile isotope [5], hence, the core geometry (e.g., fuel channels lattice pitch) must be re-optimized

for another type of fuel to obtain better neutronics performance.

### 5.6. Temperature coefficient of reactivity

To determine the temperature coefficients, the cross-section temperatures  
 310 for the fuel and moderator were changed from 900 K to 1000 K. This study considered three different cases:

1. Fuel salt temperature rising from 900 K to 1000 K.
2. Graphite temperature rising from 900 K to 1000 K.
3. Whole reactor temperature rising from 900 K to 1000 K.

### 315 5.7. Six Factor analysis

The effective multiplication factor can be expressed using the following formula:

$$k_{eff} = k_{inf}P_fP_t = \eta\epsilon pfP_fP_t$$

Table 9 summarizes the six factors for both initial and equilibrium fuel salt composition. Using SERPENT-2 built-in online reprocessing capabilities all six

Table 8: Temperature coefficients of reactivity for 3 different initial fuel salt compositions at startup and equilibrium. Confidence interval  $\pm\sigma$  for all coefficients is between 0.11 and 0.16 pcm/K).

Reactivity coefficient (pcm/K)	Startup fissile material					
	<sup>233</sup> U		Pu		TRU	
	Initial	Equil.	Initial	Equil.	Initial	Equil.
Fuel temperature	-4.96	-5.26	-4.99	-3.12	-3.23	-1.97
Fuel density	+1.49	+2.34	+1.54	-1.58	-0.37	-1.62
Total fuel	-3.77	-2.83	-3.22	-4.23	-3.25	-3.69
Graphite temperature	+1.45	+0.45	-2.68	-1.37	-1.44	-1.14
Total core	-1.77	-2.59	-6.54	-5.06	-4.79	-4.76

Table 9: Six factors for the SD-TMSR model for 3 different initial fuel salt compositions at startup and equilibrium.

Factor	Startup fissile material					
	$^{233}\text{U}$		Pu		TRU	
	Initial	Equil	Initial	Equil	Initial	Equil
$\eta$	1.26	1.40	1.66	1.44	1.57	1.31
f	0.97	0.98	0.96	0.76	0.80	0.75
p	0.54	0.43	0.26	1.60	0.17	0.15
$\epsilon$	1.49	1.67	2.45	5.87	4.83	6.81
$P_f$	0.99	0.99	0.99	0.99	0.99	0.99
$P_t$	1.00	1.00	1.00	1.00	1.00	1.00

factors and their statistical uncertainties have been calculated at the beginning of operation and after 20 years of operation. The fast and thermal non-leakage probabilities and the thermal utilization factor (f) remain constant regardless of neutron spectrum hardening during operation. In contrast, the neutron reproduction factor ( $\eta$ ), resonance escape probability ( $p$ ), and fast fission factor ( $\epsilon$ ) differ notably between initial and equilibrium state. The neutron spectrum is soft at the beginning of reactor life (Figure ??), but neutron spectrum hardening causes the fast fission factor to grow throughout the core's lifetime. Conversely, the resonance escape probability decreases during reactor operation. The neutron reproduction factor increases during reactor operation due to accumulation of fissile plutonium isotopes, which produce more neutrons per fission ( $\nu$ ). This six factors' evolution agrees with previously determined evolution parameters for a similar single-fluid double-zone MSBR [7, 30].

## 6. Conclusion

In the present paper, five different types of initial fissile materials have been studied for transitioning to thorium fuel cycle in the SD-TMSR. The molar composition of start-up fuel for all five cases is listed in Table 4, as well, the

inventories in Table 5. We adopted two different feed mechanisms; thorium feed  
mechanism and non-thorium feed mechanism. The whole-core of the SD-TMSR  
was simulated with Pu reactor-grade, TRU, and  $^{233}\text{U}$  as initial fissile materials.  
Additionally, the variation of the effective multiplication factor  $k_{eff}$ , inventory,  
and other neutronic parameters have been investigated. Results demonstrated  
that continuous flow of Pu reactor-grade helps in transition to thorium fuel  
cycle within a relatively short time ( $\approx 4.5$  years) compared to 26 years for  
Th/ $^{233}\text{U}$  start-up fuel. Meanwhile, using TRU as initial fissile materials shows  
the possibility of operating the SD-TMSR for a long period of time ( $\approx 40$  years)  
without any external feed of  $^{233}\text{U}$ . in addition, the Pu proportion in fuel salt has  
been calculated and found to be below the solubility limit. Finally, the neutron  
spectrum shift during the reactor operation for the three selected cases has been  
calculated.

## 7. Future work

## 8. Conflict of interest

The authors declare no conflict of interest.

## 9. Acknowledgments

Osama Ashraf would like to thank the Egyptian Ministry of Higher Education  
(MoHE), as well as MEPHI's Competitiveness Program for providing financial  
support for this research. The facility and tools needed to conduct this work  
were supported by MEPHI.

The authors contributed to this work as described below.

Osama Ashraf conceived and designed the simulations, wrote the paper,  
prepared figures and/or tables, performed the computation work, and reviewed  
drafts of the paper.

Andrei Rykhlevskii conceived and designed the simulations, wrote the pa-  
per, prepared figures and/or tables, performed the computation work, and

reviewed drafts of the paper. Andrei Rykhlevskii is supported by DOE ARPA-E MEITNER program award DE-AR0000983.

G. V. Tikhomirov directed and supervised the work, conceived and designed  
365 the simulations and reviewed drafts of the paper. Prof. Tikhomirov is supported  
by Rosatom, he is Deputy Director of the Institute of Nuclear Physics and  
Engineering MEPhI. Board member of Nuclear society of Russia.

Kathryn D. Huff supervised the work, conceived and contributed to conception  
of the simulations, and reviewed drafts of the paper. Prof. Huff is supported by  
370 the Nuclear Regulatory Commission Faculty Development Program, the National  
Center for Supercomputing Applications, the NNSA Office of Defense Nuclear  
Nonproliferation R&D through the Consortium for Verification Technologies and  
the Consortium for Nonproliferation Enabling Capabilities, the International  
Institute for Carbon Neutral Energy Research (WPI-I2CNER), sponsored by  
375 the Japanese Ministry of Education, Culture, Sports, Science and Technology,  
and DOE ARPA-E MEITNER program award DE-AR0000983.

This research is part of the Blue Waters sustained-petascale computing  
project, which is supported by the National Science Foundation (awards OCI-  
0725070 and ACI-1238993) and the state of Illinois. Blue Waters is a joint effort  
380 of the University of Illinois at Urbana-Champaign and its National Center for  
Supercomputing Applications

## References

- [1] DOE, US, A technology roadmap for generation iv nuclear energy systems  
(2002) 48–52.
- 385 [2] D. D. Siemer, Why the molten salt fast reactor (msfr) is the best gen iv  
reactor, Energy Science & Engineering 3 (2) (2015) 83–97.
- [3] M. Rosenthal, P. Kasten, R. Briggs, Molten-salt reactorshistory, status, and  
potential, Nuclear Applications and Technology 8 (2) (1970) 107–117.

- [4] I. Pioro, Handbook of generation IV nuclear reactors, Woodhead Publishing, 2016.
- [5] G. C. Li, P. Cong, C. G. Yu, Y. Zou, J. Y. Sun, J. G. Chen, H. J. Xu, Optimization of Th-U fuel breeding based on a single-fluid double-zone thorium molten salt reactor, Progress in Nuclear Energy 108 (2018) 144–151. doi:10.1016/j.pnucene.2018.04.017.
- URL <http://www.sciencedirect.com/science/article/pii/S0149197018300970>
- [6] A. Nuttin, D. Heuer, A. Billebaud, R. Brissot, C. Le Brun, E. Liatard, J.-M. Loiseaux, L. Mathieu, O. Meplan, E. Merle-Lucotte, et al., Potential of thorium molten salt reactorsdetailed calculations and concept evolution with a view to large scale energy production, Progress in nuclear energy 46 (1) (2005) 77–99.
- [7] A. Rykhlevskii, J. W. Bae, K. D. Huff, Modeling and simulation of online reprocessing in the thorium-fueled molten salt breeder reactor, Annals of Nuclear Energy 128 (2019) 366–379. doi:10.1016/j.anucene.2019.01.030.
- [8] E. Merle-Lucotte, D. Heuer, C. Le Brun, J. Loiseaux, Scenarios for a worldwide deployment of nuclear energy production.
- [9] B. R. Betzler, J. J. Powers, A. Worrall, Modeling and simulation of the start-up of a thorium-based molten salt reactor, in: Proc. Int. Conf. PHYSOR, 2016.
- [10] C. Zou, C. Cai, C. Yu, J. Wu, J. Chen, Transition to thorium fuel cycle for tmsr, Nuclear Engineering and Design 330 (2018) 420–428.
- [11] C. Zou, G. Zhu, C. Yu, Y. Zou, J. Chen, Preliminary study on trus utilization in a small modular th-based molten salt reactor (smtmsr), Nuclear Engineering and Design 339 (2018) 75–82.

- [12] D. Heuer, E. Merle-Lucotte, M. Allibert, M. Brovchenko, V. Ghetta, P. Rubiolo, Towards the thorium fuel cycle with molten salt fast reactors, *Annals of Nuclear Energy* 64 (2014) 421–429.
- [13] O. Ashraf, A. Smirnov, G. Tikhomirov, Modeling and criticality calculation of the molten salt fast reactor using serpent code, in: *Journal of Physics: Conference Series*, Vol. 1189, IOP Publishing, 2019, p. 012007.
- [14] O. Ashraf, A. Smirnov, G. Tikhomirov, Nuclear fuel optimization for molten salt fast reactor, in: *Journal of Physics: Conference Series*, Vol. 1133, IOP Publishing, 2018, p. 012026. doi:doi:10.1088/1742-6596/1133/1/012026.
- [15] C. Fiorina, M. Aufiero, A. Cammi, F. Franceschini, J. Krepel, L. Luzzi, K. Mikityuk, M. E. Ricotti, Investigation of the msfr core physics and fuel cycle characteristics, *Progress in Nuclear Energy* 68 (2013) 153–168.
- [16] C. de Saint Jean, M. Delpech, J. Tommasi, G. Youinou, P. Bourdot, Scénarios cne: réacteurs classiques, caractérisation à l’équilibre, rapport CEA DER/SPRC/LEDC/99-448.
- [17] M. Jiang, H. Xu, Z. Dai, Advanced fission energy program-tmsr nuclear energy system, *Bull. Chin. Acad. Sci* 27 (3) (2012) 366–374.
- [18] X. Li, X. Cai, D. Jiang, Y. Ma, J. Huang, C. Zou, C. Yu, J. Han, J. Chen, Analysis of thorium and uranium based nuclear fuel options in fluoride salt-cooled high-temperature reactor, *Progress in Nuclear Energy* 78 (2015) 285–290.
- [19] G. Li, Y. Zou, C. Yu, et al., Model optimization and analysis of th-u breeding based on msfr, *Nucl. Tech* 40 (2017) 020603–020603.
- [20] R. C. Robertson, Conceptual Design Study of a Single-Fluid Molten-Salt Breeder Reactor., Tech. Rep. ORNL-4541, comp.; Oak Ridge National Laboratory, Tenn. (Jan. 1971).  
URL <http://www.osti.gov/scitech/biblio/4030941>



- 445 [21] J. C. Marka, Explosive properties of reactor-grade plutonium, *Science & Global Security* 4 (1) (1993) 111–128.
- [22] N. OECD, Probabilistic safety assessment in nuclear power plant management: a report by a group of experts of the nea committee on the safety of nuclear installations, june 1989, 112 (1989).
- 450 [23] J. Serp, M. Allibert, O. Beneš, S. Delpech, O. Feynberg, V. Ghetta, D. Heuer, D. Holcomb, V. Ignatiev, J. L. Kloosterman, et al., The molten salt reactor (msr) in generation iv: overview and perspectives, *Progress in Nuclear Energy* 77 (2014) 308–319.
- 455 [24] J. Leppänen, M. Pusa, T. Viitanen, V. Valtavirta, T. Kaltiaisenaho, The serpent monte carlo code: Status, development and applications in 2013, in: *SNA+ MC 2013-Joint International Conference on Supercomputing in Nuclear Applications+ Monte Carlo*, EDP Sciences, 2014, p. 06021.
- [25] M. Aufiero, A. Cammi, C. Fiorina, J. Leppänen, L. Luzzi, M. E. Ricotti, An extended version of the serpent-2 code to investigate fuel burn-up and core material evolution of the molten salt fast reactor, *Journal of Nuclear Materials* 441 (1-3) (2013) 473–486.
- 460 [26] A. Isotalo, M. Pusa, Improving the accuracy of the chebyshev rational approximation method using substeps, *Nuclear Science and Engineering* 183 (1) (2016) 65–77.
- 465 [27] V. Ignatiev, O. Feynberg, A. Merzlyakov, A. Surenkov, A. Zagnitko, V. Afonichkin, A. Bovet, V. Khokhlov, V. Subbotin, R. Fazilov, et al., Progress in development of mosart concept with th support, in: *Proceedings of ICAPP*, Vol. 12394, 2012.
- [28] D. Sood, P. Iyer, R. Prasad, V. Vaidya, K. Roy, V. Venugopal, Z. Singh, M. Ramaniah, Plutonium trifluoride as a fuel for molten salt reactors-solubility studies, *Nuclear technology* 27 (3) (1975) 411–415.
- 470

- [29] O. Ashraf, A. Rykhlevskii, G. Tikhomirov, K. D. Huff, Whole core analysis of the single-fluid double-zone thorium molten salt reactor (sd-tmsr), *Annals of Nuclear Energy*.
- [30] J. Park, Y. Jeong, H. C. Lee, D. Lee, Whole core analysis of molten salt breeder reactor with online fuel reprocessing, *International Journal of Energy Research* 39 (12) (2015) 1673–1680. doi:10.1002/er.3371.  
URL <http://doi.wiley.com/10.1002/er.3371>